CAV2021
11th International Symposium on Cavitation
May 10-13, 2021, Daejon, Korea

Laser-Induced Cavitation Near a Concave Surface

Tomaž Požar, Vid Agrež and Rok Petkovšek*

Faculty of Mechanical Engineering, University of Ljubljana, Slovenia

Abstract: We report on the dynamics of the cavitation bubble and shock waves generated in water by an optical breakdown near a concave solid surface. In contrast to the presence of other geometries like plane or convex boundaries, that upon reflection do not modify the initially divergent nature of the emitted shock waves, the presence of a concave boundary introduces a novel effect with striking consequences: refocusing of an initially divergent shock wave capable of causing secondary cavitation. A human eye phantom, mimicking a biological structure, is employed, where the acoustic focusing is mediated by the concave surface of a cornea-shaped spherical acoustic reflector. To visualize the shock wave propagation and cavitation dynamics, we used a combination of a fast or a still camera with an adaptive pulsed illumination employing either schlieren technique or shadow cinematography. The acoustic refocusing and the generation of the aggregates of secondary cavities near the acoustic focal volume are specific for optically generated bubbles near a concave surface. It was found that the first collapse shock wave induces the strongest secondary cavitation. The implications extend from medicine to any technology that deals with cavitation near inward curved surfaces such as cavitation peening and cavitation erosion.

Keywords: concave surface; optical breakdown; acoustic focusing; secondary cavitation; shock waves

1. Introduction

This contribution reports on the visualization of the intricate dynamics and interplay of the cavitation bubble and multiple shock waves generated in water by a localized, laser-induced breakdown near a concave solid surface. In contrast to the presence of other geometries like plane [1–3] or convex boundaries [1,4] that upon reflection do not modify the initially divergent nature of the emitted shock waves, the presence of a concave boundary [1,5–7] introduces an additional effect with striking consequences: refocusing of an initially divergent shock wave capable of causing secondary cavitation [7].

To demonstrate the effects following the laser-generated breakdown in the vicinity of an inward curved boundary, we chose a human eye phantom where the acoustic focusing is mediated by the concave surface of a cornea-shaped circular acoustic reflector. To some extent, the experiments thus strive to mimic the transient response of an actual human eye after the application of a laser pulse causing localized ionization on the optical axis within the eye.

The present experiments visualize the evolution of the cavitation bubble and shock waves in the first millisecond after the application of a laser pulse typically used in medical procedures in experimental configuration simulating human eye. Due to such a fast dynamics, plethora of cavitation bubble-shock wave interactions within this time period could potentially influence the treatment of various pathologies in ophthalmology. In order to assess the invasiveness of such medical treatments and potentially to improve existing procedure, it is important to understand what is going on in the first millisecond just after the optical breakdown in a geometry confined by shock wave focusing surfaces.

* Corresponding Author: Rok Petkovšek, rok.petkovsek@fs.uni-lj.si

2. Materials and Methods

To visualize the shock wave propagation and cavitation bubble dynamics, we used a combination of a fast or a still camera with an adaptive pulsed illumination employing either schlieren technique or shadow cinematography [8]. The experiments were performed at 23 °C and unreduced pressure of 97.6 kPa. The main constituents used in the central part of the experiment are: water, ophthalmic lens and water tank as illustrated in Figure 1. The latter are made of poly(methyl methacrylate) (PMMA). The contacting surface of the ophthalmic lens (Capsulotomy lens K30-1120, Katena Products, USA) has a measured curvature of 8.1 mm. A signal generator was used to trigger the excitation laser with a frequency of 0.2 Hz. Optical breakdown was achieved with a Q-switched Nd:YAG laser similar in performance to typical medical photodisruptors used in ophthalmology. It emits laser pulses at the wavelength of 1064 nm with an energy of 15 mJ. The photodiode was used to register the transmitted excitation pulse and trigger both, the adaptive illumination system and the image acquisition system.

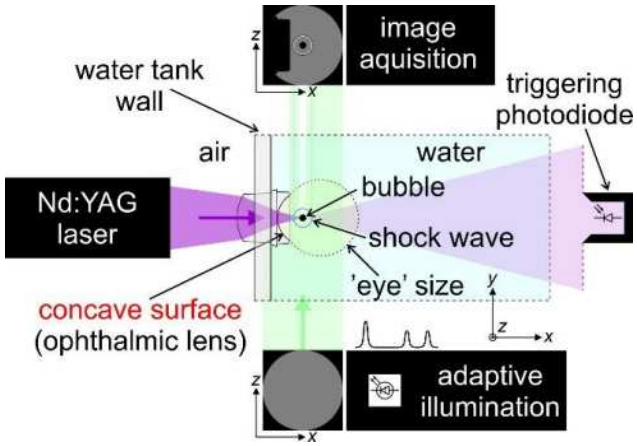

Figure 1. Experimental setup. The central part of the experiment in shown in the top view, while the excitation beam profile of the illumination pulse and the image on the detector are presented in the side view. The magenta-colored area represents the path of the excitation pulse, while the green-colored area gives the path of the illumination pulse. The cavitation bubble (the black disk), the breakdown shock wave (the blue circle) and the ophthalmic lens deflect the illumination pulse and form the shadow image. For comparison, the approximate dimensions of the human eye in contact with the ophthalmic lens are shown by the yellow colored area.

The collimated 1-inch-diameter background illumination was produced by an adaptable, laser-diode-based illumination system which was developed to simultaneously visualize the dynamics of slow and fast phenomena in optically transparent media. The system can be coupled with still or high-speed cameras and makes it possible to generate an arbitrary train of illumination pulses with a variable pulse duration, pulse energy, and an intrapulse delay with a temporal resolution of 12.5 ns.

Two high-speed visualization techniques were used in the experiments: shadowgraphy and schlieren with the knife-edge set in the vertical position. The shadowgraphy was combined with the still camera (standard 2M pixels industrial camera) and a single illumination pulse with a variable delay between the breakdown and the illumination pulse. Single frames of successive repeatable breakdown events were imaged with time increments of 125 ns yielding a series of multiple-event frames to simulate a single event. True, single event visualization was performed in the schlieren mode with the synchronization of the fast-camera (Fastcam SA-Z 2100K, Photron, Japan) and the illumination system. The fast-camera was running with a 210 kfps (kilo frames per second) frame rate and the illumination system gave one illumination pulse per frame.

* Corresponding Author: Rok Petkovšek, rok.petkovsek@fs.uni-lj.si

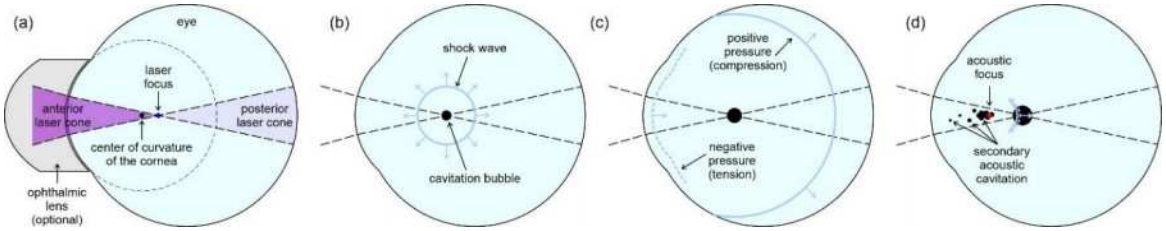

Figure 2. Shock wave refocusing.

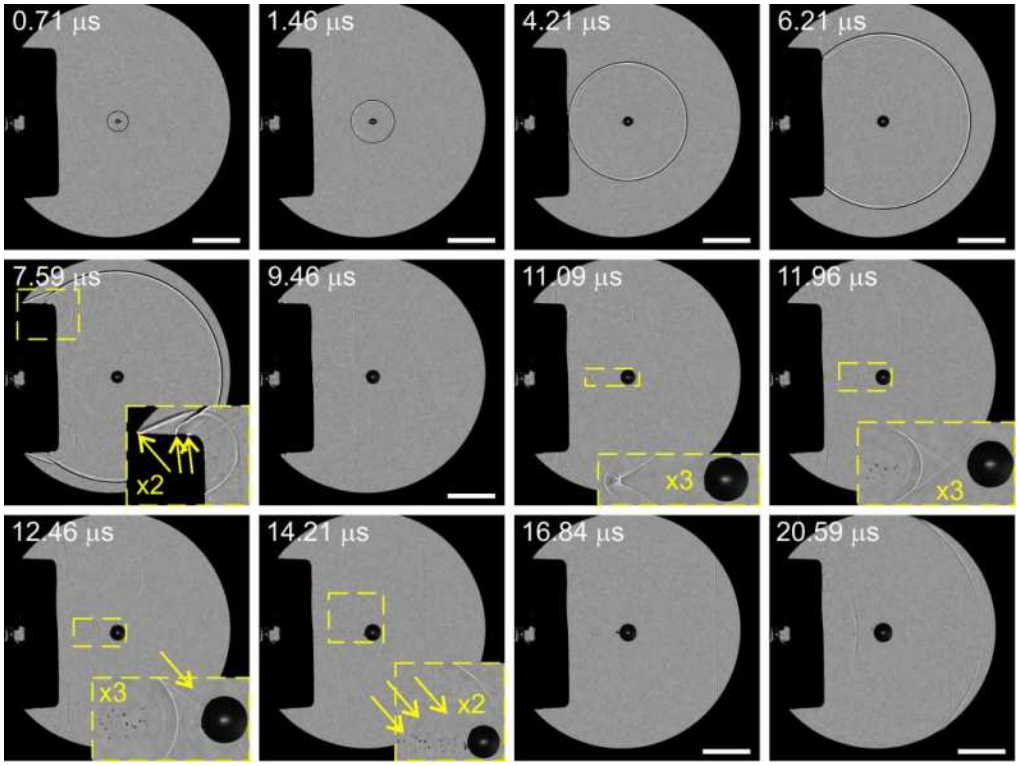

Figure 3. Twelve shadowgrams showing the consequences of the presence of the concave surface on the propagation of laser-induced shock waves. The yellow arrows guide the eye to interesting features. The time after the optical breakdown is given in the upper-left corner, while the yellow dashed rectangles mark the zoom in areas given in the bottom-right corner of a few selected shadowgrams. White bar: 5 mm.

3. Results

The most important aspects of the shock wave refocusing mechanism in a human eye (or in general near a concave surface) are sketched in Figure 2. In Figure 2(a), a simplified side view of the eye depicts the optional ophthalmic lens placed on the cornea. A laser pulse is focused within the eye either directly or through the transparent ophthalmic lens. Its path forms two cones, one in front of the focus and the other one behind it. Breakdown occurs in the optical focus. Laser light is transmitted past the focus only until dense plasma is formed in the very beginning of the pulse, therefore more laser energy is absorbed in the anterior cone (darker magenta) compared to the posterior cone (paler magenta). Figure 2(b) shows the emitted spherical shock wave and the expanding cavitation bubble, generated in the optical focus. When the shock wave reaches the cornea-air or cornea-lens interface, the compressional wave reflects either as a rarefaction and changes its phase (example: cornea-air) or it remains a compression (example: cornea-lens) depending on the acoustic impedances of both media. Figure 2(c) shows the reflection of the shock wave

* Corresponding Author: Rok Petkovšek, rok.petkovsek@fs.uni-lj.si

from the cornea-air interface, where the positive pressure is marked by a solid line and negative pressure by a dashed line. After the reflected shock wave passes the acoustic focus, secondary cavitation takes place in its vicinity [Figure 2(d)]. The secondary cavitation is primarily confined to the anterior laser cone, because the threshold for the incipience of acoustic cavitation is lower in this volume due to prior absorption of laser light on the impurities. The threshold for secondary cavitation depends largely on the peak negative pressure. After the first collapse of the main bubble, the dynamics is repeated [Figures 2(b)–2(d)]. After the passage of the reflected shock wave over the anterior laser cone, smaller bubbles reappear at the same locations as initially, this time larger in size.

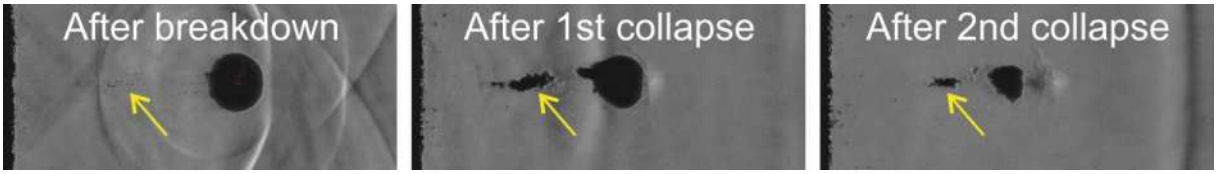

Figure 4. Intensity of the secondary cavitation.

The details of the above general description can be observed in the twelve representative multiple-event shadowgrams (Figure 3) revealing the shock wave propagation, reflection, mode-conversion, focusing and scattering, taken soon after the optical breakdown at a breakdown distance 10.13 mm ($\gamma = 5.7$) from the apex of the concave surface at twelve time instants. Further schlieren images shown in figure 4 disclose that the first collapse shock wave induces the strongest secondary cavitation, followed by the second collapse shock wave and then the breakdown shock wave whose effect is the least pronounced. To conclude, the implications of this work extend from ophthalmology, the mock-up attempt treated here, to any technology that deals with cavitation near inward curved, conically depressed surfaces such as cavitation peening and cavitation erosion.

Acknowledgments: The authors acknowledge the financial support from the Slovenian Research Agency (research core Funding No. P2-0270 and Project Nos. L2-8183, L2-9240 and L2-9254).

References

1. Tomita, Y.; Robinson, P.B.; Tong, R.P.; Blake, J.R. Growth and collapse of cavitation bubbles near a curved rigid boundary. *J. Fluid Mech.* **2002**, *466*, 259-283.
2. Dular, M.; Požar, T.; Zevnik, J.; Petkovšek, R. High speed observation of damage created by a collapse of a single cavitation bubble. *Wear* **2019**, *418–419*, 13–23.
3. Lauterborn, W.; Kurz, T.; Mettin, R.; Ohl, C.D. Experimental and Theoretical Bubble Dynamics. In *Advances in Chemical Physics*; Prigogine, I.; Rice, S.A., Eds.; John Wiley & Sons, New York, USA, 1999; Volume 110, pp. 295–380.
4. Zevnik, J.; Dular, M. Cavitation bubble interaction with a rigid spherical particle on a microscale. *Ultrason. Sonochem.* **2020**, *69*, 105252.
5. Cui, P.; Wang, S.P.; Zhang, A.M.; Liu, Y.L. Spark Bubble Collapse near Non-flat Surfaces. In Proceedings of the 10th Symposium on Cavitation (CAV2018), Katz, J., Eds.; ASME Press, Baltimore, Maryland, USA, May 14–16, 2018; pp. 1-4.
6. Shervani-Tabar, M.T.; Rouhollahi, R. Numerical study on the effect of the concave rigid boundaries on the cavitation intensity. *Sci. Iran* **2017**, *24*, 1958-1965.
7. Požar, T.; Petkovšek, R. Cavitation induced by shock wave focusing in eye-like experimental configurations. *Biomed. Opt. Express* **2020**, *11*, 432-447.
8. Agrež, V.; Požar, T.; Petkovšek, R. High-speed photography of shock waves with an adaptive illumination. *Opt. Lett.* **2020**, *45*, 1547–1550.

* Corresponding Author: Rok Petkovšek, rok.petkovsek@fs.uni-lj.si